THE JOURNAL OF BIOLOGICAL CHEMISTRY VOL. 289, NO. 2, pp. 803–813, January 10, 2014

A New Paradigm for Enzymatic Control of α-Cleavage and β-Cleavage of the Prion Protein*

Received for publication, July 15, 2013, and in revised form, November 6, 2013 Published, JBC Papers in Press, November 18, 2013, DOI 10.1074/jbc.M113.502351

Alex J. McDonald, Jessie P. Dibble, Eric G. B. Evans, and Glenn L. Millhauser[1]

From the Department of Chemistry and Biochemistry, University of California, Santa Cruz, California 95064

Background: The prion protein (PrP) is cleaved into bioactive fragments by enzymes and metal catalysis.
Results: Key members of the ADAM protease family yield all observed PrP products.
Conclusion: Proteases alone may be responsible for PrP processing, with distinct activities depending on specific enzymes.
Significance: Elucidation of the responsible enzymes and products can be used to evaluate PrP function and proteolysis in prion disease.

The cellular form of the prion protein (PrP^C) is found in both full-length and several different cleaved forms *in vivo*. Although the precise functions of the PrP^C proteolytic products are not known, cleavage between the unstructured N-terminal domain and the structured C-terminal domain at Lys-109 ↓ His-110 (mouse sequence), termed α-cleavage, has been shown to produce the anti-apoptotic N1 and the scrapie-resistant C1 peptide fragments. β-Cleavage, residing adjacent to the octarepeat domain and N-terminal to the α-cleavage site, is thought to arise from the action of reactive oxygen species produced from redox cycling of coordinated copper. We sought to elucidate the role of key members of the ADAM (a disintegrin and metalloproteinase) enzyme family, as well as Cu^{2+} redox cycling, in recombinant mouse PrP (MoPrP) cleavage through LC/MS analysis. Our findings show that although Cu^{2+} redox-generated reactive oxygen species do produce fragmentation corresponding to β-cleavage, ADAM8 also cleaves MoPrP in the octarepeat domain in a Cu^{2+}- and Zn^{2+}-dependent manner. Additional cleavage by ADAM8 was observed at the previously proposed location of α-cleavage, Lys-109 ↓ His-110 (MoPrP sequencing); however, upon addition of Cu^{2+}, the location of α-cleavage shifted by several amino acids toward the C terminus. ADAM10 and ADAM17 have also been implicated in α-cleavage at Lys-109 ↓ His-110; however, we observed that they instead cleaved MoPrP at a novel location, Ala-119 ↓ Val-120, with additional cleavage by ADAM10 at Gly-227 ↓ Arg-228 near the C terminus. Together, our results show that MoPrP cleavage is far more complex than previously thought and suggest a mechanism by which PrP^C fragmentation responds to Cu^{2+} and Zn^{2+}.

The prion protein (PrP)[2] is an abundant extracellular glycosylphosphatidylinositol (GPI)-anchored glycoprotein consisting of a helical C-terminal domain and a partially structured N-terminal domain (Fig. 1) (1, 2). Prion diseases, which result from conversion of cellular PrP (PrP^C) to the misfolded aggregated scrapie form (PrP^{Sc}), include Creutzfeldt-Jakob disease and kuru in humans, bovine spongiform encephalopathy, chronic wasting disease in deer and elk, and scrapie in goats and sheep (3, 4). The full-length protein is ~210 amino acids long, but PrP^C is also found in several distinct truncated forms *in vivo*, with proteolytic species possessing unique bioactive properties (5, 6).

In healthy tissues, enzyme cleavage of PrP^C at approximately Lys-109 ↓ His-110 (mouse sequence), termed α-cleavage, produces the N- and C-terminal fragments, N1 and C1, respectively. The preponderance of recent evidence suggests that α-cleavage, which separates most of the PrP N terminus from the folded C terminus, is due to action from one or more members of the ADAM (a disintegrin and metalloproteinase) family of enzymes, specifically ADAM8, ADAM10, and ADAM17 (7, 8). α-Cleavage was originally assigned to ADAM10, but recent studies found that neither knocking out ADAM10 nor treatment with ADAM10-specific protease inhibitors is capable of blocking α-cleavage and instead blocks proteolysis of PrP^C near the C-terminal GPI anchor at Gly-227 ↓ Arg-228 (9–11). More recently, ADAM8 was identified as the protease responsible for α-cleavage in skeletal muscle tissue (7). Interestingly, a study aimed at identifying the specific α-cleavage site found that PrP^C exhibits remarkable tolerance to point mutations and deletions of short segments (12). Deletion of the extended segment 100–129 was necessary to fully block cleavage.

The prodomains released by α-cleavage exhibit potent activities. The N1 fragment is anti-apoptotic, possibly acting through the inhibition of caspase-3 (13). Conversely, the C1 fragment promotes apoptosis through p53-dependent caspase-3 activity, although it appears as though the protective effects of N1 significantly outweigh the pro-apoptotic effects of C1 (14). Perhaps more importantly, substoichiometric levels of C1 protect against PrP^{Sc} propagation (15, 16).

In Creutzfeldt-Jakob disease patients, postmortem brain homogenates present a second cleavage site, termed β-cleavage, which produces N2 and C2 fragments (6). Because the C2 fragment from the homogenates is proteinase K-resistant and migrates the same distance upon gel electrophoresis as the proteinase K-digested PrP^{Sc} core (proteinase K-resistant PrP), it was originally proposed that the observed C2 fragment from

* This work was supported, in whole or in part, by National Institutes of Health Grant GM065790.
[1] To whom correspondence should be addressed. Tel.: 831-459-2176; Fax: 831-459-2935; E-mail: glennm@ucsc.edu.
[2] The abbreviations used are: PrP, prion protein; PrP^C, cellular PrP; PrP^{Sc}, scrapie PrP; $MoPrP^C$, recombinant mouse PrP^C; GPI, glycosylphosphatidylinositol; ROS, reactive oxygen species; Aβ, amyloid-β.

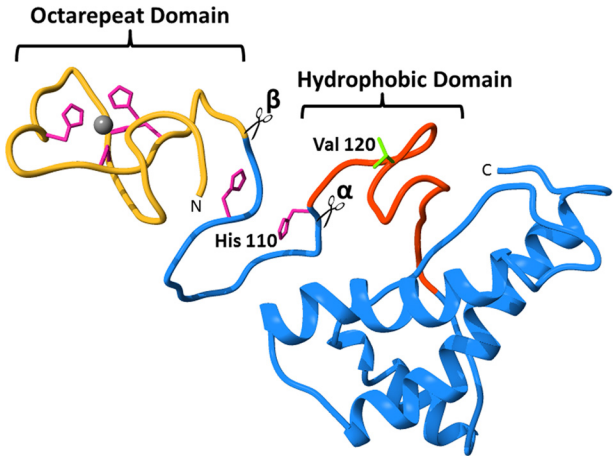

FIGURE 1. **Model of MoPrP with amino acids and domains implicated in cleavage of PrP^C.** The octarepeat domain (*gold*) coordinates Cu^{2+} and Zn^{2+} through four histidines (*magenta*). There are two additional Cu^{2+}-coordinating histidine residues outside the octarepeat domain at positions 95 and 110 (*magenta*). The central hydrophobic domain (*orange*) connects the unstructured N-terminal region to the structured C-terminal domain. The previously proposed sites for α- and β-cleavage are indicated at the beginning of the hydrophobic domain and at the end of the octarepeat domain, respectively.

Creutzfeldt-Jakob disease brain tissue corresponded to proteinase K-resistant PrP, placing β-cleavage at Gly-89 ↓ Gln-90. Subsequently, a soluble cleavage fragment of PrP^C determined by antibody staining to be similar to C2 was observed in scrapie-free CHO and SH-SY5Y cell lines expressing PrP^C (17, 18). The observed levels of C2 are greatly enhanced upon addition of H_2O_2, suggesting proteolysis by reactive oxygen species (ROS) generated by intrinsic copper, which binds with high affinity to the N-terminal octarepeats (residues 60–91, human sequence). However, there have been several recent studies implicating proteases from the calpain and cathepsin families in β-cleavage of PrP^{Sc}, leaving open the possibility that β-cleavage in PrP^C could also be enzymatic (19, 20). Unlike the N1 and C1 fragments, N2 and C2 do not show any bioactivity or neuroprotection, although β-cleavage production of N2 and C2 may indirectly assert a biological effect by denying the formation of N1 and C1 (13–15).

PrP^C is enzymatically shed from its GPI membrane attachment by the action of ADAM10 (10). Free PrP^C is found in cell culture and human cerebral spinal fluid. Recent literature suggests several possible functions for PrP^C, distinct from its N1 and C1 fragments. For example, full-length PrP^C may trap pre-amyloid-β (Aβ) oligomers, implicated in Alzheimer disease, in its hydrophobic segment, thereby acting in defense against neurodegenerative disease (21). In addition, membrane-bound PrP^C stimulates NMDA receptors (22), an activity that may be down-regulated by release through a sheddase. Finally, full-length PrP^C, but not its N- or C-terminal segment, promotes neuron differentiation and growth, suggesting a role in neurological development (23).

The prevailing paradigm of PrP^C cleavage posits that α-cleavage and sheddase events are enzymatically driven and constitute normal processing. However, β-cleavage results from aberrant copper redox activity and is associated with the development of prion disease. Recent work from our laboratory (24) identified a metal ion-driven tertiary structure between the PrP^C N- and C-terminal domains, thereby suggesting a re-evaluation of the relative roles of ADAM proteases and copper and zinc in proteolysis. Using Zn^{2+}, which is both a natural PrP^C-binding metal and a surrogate for Cu^{2+}, Spevacek *et al.* (24) found that the metal-occupied octarepeat domain makes contact with the C-terminal surface formed by helices 2 and 3. This interaction is systemically weakened by familial mutations within these two helices. The compact protein resulting from this newly identified contact likely restricts conformational freedom of the proteolytically susceptible linker (residues 91–125), which encompasses the α-cleavage site.

In this work, we use LC/MS to examine the relative activities of ADAM8, ADAM10, and ADAM17 on recombinant mouse PrP^C ($MoPrP^C$) in the absence and presence of both Zn^{2+} and Cu^{2+}. We show that Cu^{2+}-generated ROS, ADAM8, ADAM10, and ADAM17 are all capable of cleaving MoPrP, albeit at distinct locations. Surprisingly, we observed that in the absence of ROS, ADAM8 cleaved $MoPrP^C$ at both α- and β-cleavage locations in a Cu^{2+}- and Zn^{2+}-dependent manner. Moreover, we found that α-cleavage occurred at several nearby locations depending on the specific enzyme and condition. Through our assay, we were able to design mutants that block certain cleavage events by ADAM8, ADAM10, and ADAM17, an advance that could prove useful in further analysis of the role of enzymes in PrP^C function and prion disease. Finally, we observed that the familial mutants show altered α-cleavage profiles. As opposed to metal-catalyzed backbone scission, our findings suggest a new paradigm whereby physiologic metal ions regulate enzyme-driven PrP^C processing, controlling the relative α- and β-cleavage products.

EXPERIMENTAL PROCEDURES

Protein Expression—The prion protein was expressed and purified as described previously (25). In brief, MoPrP(23–230) was cloned into the pET101 vector using the Champion™ pET101 Direction TOPO® expression kit (Invitrogen). Mutant constructs were made with the pET101-MoPrP(23–230) plasmid as the template using the GeneArt® site-directed mutagenesis kit (Invitrogen). All constructs were verified by DNA sequencing. The pET101 vector was then transformed into BL21 Star™ cells and expressed for 20 h via autoinduction (26). Cells were lysed, and inclusion bodies containing MoPrP were purified from the lysate. All constructs were then purified with an ÄKTA purifier (GE Healthcare) using a Ni^{2+} immobilized metal ion affinity column with the exception of MoPrP(90–230), which was purified using a Q-Sepharose anion exchange column. Protein was eluted from the Ni^{2+} immobilized metal ion affinity column with 8 M guanidine HCl (pH 4.5) while monitoring A_{280}. Fractions spanning the elution peak were combined, and the pH was raised to 8, followed by storage at 4 °C for 2 days to facilitate proper folding. The protein was then purified by reverse-phase HPLC using a C_4 column (Grace/Vydac), and the correct mass of the purified protein was verified by electrospray ionization mass spectrometry. Fractions containing the purified protein were pooled, lyophilized, and stored at −20 °C for future use. Protein stocks were reconstituted in 0.2-μm filtered water and quantified with a NanoDrop UV-visible spectrometer (Thermo Scientific) prior to use.

Cleavage of MoPrP by ROS—Cleavage of MoPrP was carried out by forming ROS *in vitro* using ascorbic acid and Cu^{2+}. 50-μl samples were made containing 100 μM MoPrP, 25 mM MOPS (pH 7.4), and 1 mM ascorbic acid. To begin the reaction, $Cu(OAc)_2$ was added to a final concentration of 200 μM. For control samples, Cu^{2+} was omitted from the reaction, resulting in no cleavage. Although the above conditions produced cleavage of MoPrP within the octarepeats, it was difficult to identify peaks by mass spectroscopy due to excessive oxidation from H_2O_2 generated by Cu^{2+}/ascorbic acid redox cycling. To alleviate excessive oxidation, the H_2O_2 decomposition enzyme catalase (Spectrum) was added to the reaction to a final concentration of 0.1 mg/ml. Samples were allowed to incubate overnight at 25 °C. Once the reaction was completed, it was quenched using the free radical scavenger dimethyl sulfoxide, which was added to a final concentration of 1%.

ADAM8 Cleavage of MoPrP—Recombinant human ADAM8 was purchased from R&D Systems. ADAM8 must be activated before use by cleaving a propeptide with thermolysin. First, a fresh stock of 1.5 μg/ml thermolysin was made with ADAM8 primary buffer (50 mM Tris, 10 mM $CaCl_2$, and 150 mM NaCl (pH 7.5)), and separately, a 0.5 mM stock of the thermolysin inhibitor phosphoramidon (Santa Cruz Biotechnology) was made with ADAM8 primary buffer. Recombinant ADAM8 was diluted to 400 μg/ml in ADAM8 primary buffer, and then an equal volume of 1.5 μg/ml thermolysin stock was added. The mixture was incubated at 37 °C for 30 min, and the reaction was stopped by the addition of phosphoramidon to a final concentration of 0.05 mM and incubated at 25 °C for 15 min. Thorough controls were performed to ensure that this process fully inactivated thermolysin (data not shown). Before use, the activated ADAM8 was diluted 5-fold with dilution buffer (20 mM Tris, 5 mM $CaCl_2$, and 25 mM KCl (pH 7.4)). Separately, working stocks of 40 μM MoPrP constructs were made from lyophilized protein brought up in dilution buffer and quantified by UV-visible spectroscopy. For reactions testing the effects of Cu^{2+} or Zn^{2+} on ADAM8 cleavage, the appropriate molar equivalents of $Cu(OAc)_2$ or $ZnCl_2$ were added to the 40 μM MoPrP solutions, followed by incubation at 25 °C for 15 min. It is important to use the low salt dilution buffer, or MoPrP will precipitate out of solution in the presence of Cu^{2+} or Zn^{2+}. 15 μl of dilute activated ADAM8 and 15 μl of MoPrP construct were combined and allowed to react for 6 h at 37 °C unless noted otherwise. The reaction was stopped by the addition of 5 μl of 1% formic acid and stored at 4 °C until assayed. For the time trial of ADAM8 activity on MoPrP, the reaction was quenched at each time point by the addition of the metalloproteinase inhibitor Batimastat to a final concentration of 5 μM and then stored at 4 °C until assayed.

ADAM10 and ADAM17 Cleavage of MoPrP—Recombinant human ADAM10 and ADAM17 were purchased from R&D Systems. ADAM10 was diluted to 2 ng/μl in ADAM10 assay buffer (25 mM Tris, 2.5 μM $ZnCl_2$, and 0.005% Brij-35 (pH 7.4)), and ADAM17 was diluted to 0.5 ng/μl in ADAM10 assay buffer. MoPrP constructs were diluted to 40 μM in ADAM10 assay buffer. 15 μl of diluted ADAM10 or ADAM17 was combined with 15 μl of MoPrP construct and incubated overnight at 37 °C. Cleavage reactions were stopped by the addition of 1 μl of 1% formic acid and stored at 4 °C until assayed.

LC/MS—MoPrP cleavage samples were spun down for 5 min at 13,000 relative centrifugal force to pellet any debris and material that may have precipitated during sample preparation. 30 μl of supernatant was then pipetted into autosampler vials and loaded into an LTQ orbitrap LC/MS autosampler (Fisher), chilled to 4 °C. 20 μl of cleavage products was drawn from a vial and separated with a C_4 HPLC column (Higgins Analytical) using a 60-min gradient of water/acetonitrile mobile phases. The A_{280} was continuously recorded by a photodiode array, whereas mass spectra were continuously taken using an LTQ orbitrap mass spectrometer (Fisher). The C_4 column was flushed with 95% acetonitrile to remove any residually bound protein and then re-equilibrated with 95% water between each sample run.

Cleavage Product Identification and Analysis—The LC/MS spectra from each sample run were first analyzed by MS Bioworks. The mass spectrum ladder for each peak separated by the C_4 column was deconvoluted using Bioworks to reveal the parent mass of the cleavage product (data not shown). The masses of the observed peaks were cross-referenced against the predicted masses of hydrolysis of all possible peptide bonds of MoPrP to determine which potential cleavage fragment each observed peak corresponded to. For all cleavage fragments enzymatically produced, observed masses were within 1 atomic mass unit of the mass of a predicted cleavage fragment. Fragments produced by ROS tended to show one or more oxidations. Once peaks were annotated with the cleavage fragment that produced them, the A_{280} of each peak was separately integrated in Xcalibur (Thermo Scientific), ensuring that integration spanned the retention time range corresponding to the proper fragment mass. Peak integrals were then divided by the extinction coefficient of their corresponding fragment to give relative abundance. Error bars shown for the Cu^{2+} titration of ADAM-PrP cleavage ($n = 3$) are representative of the reproducibility of LC/MS cleavage assays, typically within 10% error (see Fig. 4, *A* and *B*).

RESULTS

ROS Generated from Cu^{2+} Redox Cycling Are Capable of Cleaving MoPrP within the Octarepeat Domain—In vivo work has established that Cu^{2+}-generated ROS are a mechanism underlying β-cleavage of PrP^C (17); however, the location of the cleavage site has only been approximated by Western blot analysis (6). To further understand the physiological events leading to N2 and C2 production, we sought to first determine the precise location of ROS-driven β-cleavage *in vitro*. Copper and the naturally occurring reductant ascorbic acid produce hydroxyl radicals ($HO^•$), a common component of ROS. Copper acetate and ascorbic acid at concentrations of 200 μM and 100 mM, respectively, were added to a solution of 100 μM MoPrP and reacted overnight. To avoid spurious oxidation events at amino acid side chains, we also included catalase, which rapidly inactivates excess H_2O_2 but not $HO^•$. As shown in Fig. 2, LC/MS revealed a clear C2 fragment, along with multiple N-terminal peptides. Evaluation of the N2 products showed that MoPrP was cleaved following each of the four histidines

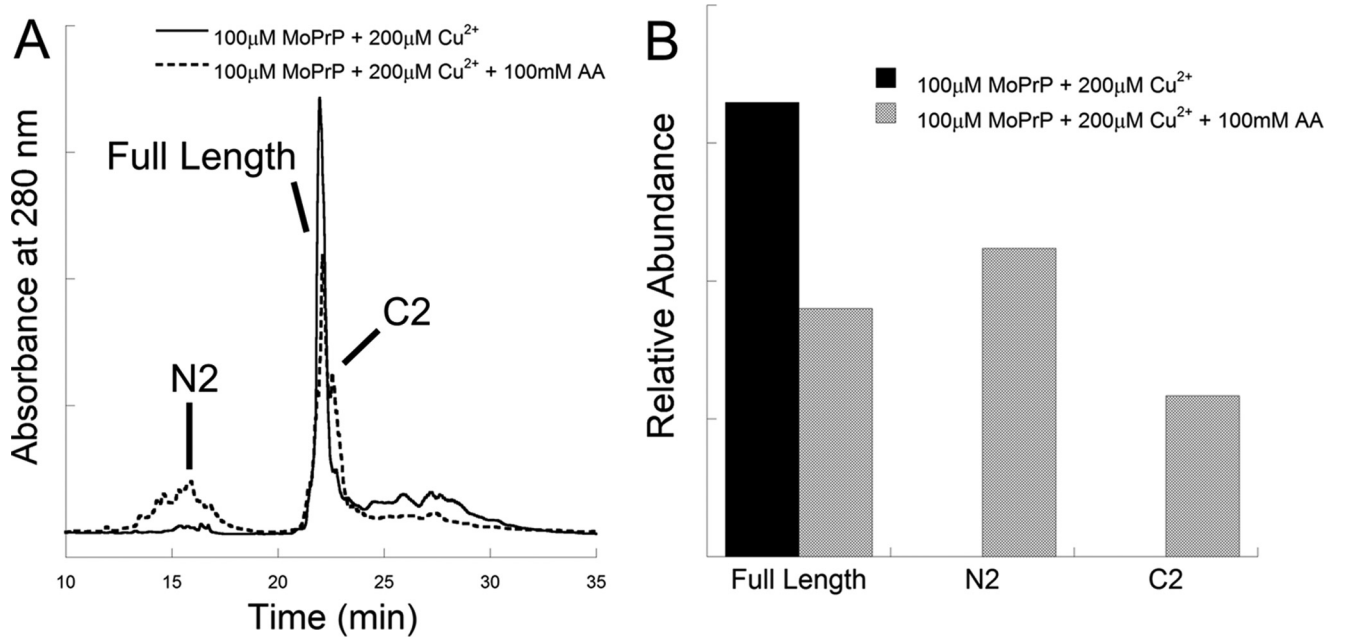

FIGURE 2. **Redox cycling of Cu^{2+} coordinated to MoPrP is capable of producing β-cleavage fragments.** 100 μM MoPrP was incubated with 2 eq of Cu^{2+} in the absence or presence of 100 mM ascorbic acid (*AA*) overnight and then assayed by LC/MS. The resulting redox cycling of Cu^{2+} produced ROS capable of cleaving MoPrP following the four histidines of the N-terminal octarepeat domain (His-60 ↓ Gly-61, His-68 ↓ Gly-69, His-76 ↓ Gly-77, and His-84 ↓ Gly-85). *A*, peaks corresponding to the N- and C-terminal fragments were identified in the LC trace of MoPrP with 2 eq of Cu^{2+} and 100 mM ascorbic acid (*dashed line*) but were not seen in the absence of ascorbic acid (*solid line*). *B*, significant peaks from the LC trace were identified by mass spectrometry and then integrated to determine the relative abundance of the peptide fragments. The four N-terminal fragments produced from cleavage at each histidine in the octarepeats co-eluted and were integrated together as N2. Likewise, the four complementary C-terminal fragments co-eluted as a distinct shoulder of the peak for full-length protein and were integrated together as C2.

coordinated to Cu^{2+} within the octarepeat domain with equal likelihood (His-60 ↓ Gly-61, His-68 ↓ Gly-69, His-76 ↓ Gly-77, and His-84 ↓ Gly-85), but not at the previously proposed site of β-cleavage, Gly-89 ↓ Gln-90 (6). *In vivo*, cellular binding partners of PrP^C may cause β-cleavage to be favored at one octarepeat domain histidine over the others. When ascorbic acid was omitted from the reaction, no cleavage was observed (Fig. 2). These data suggest that ROS-mediated cleavage does not provide a clean separation between the intact N2 and C2 fragments but instead processes N-terminal PrP at multiple locations.

MoPrP Is Cleaved by ADAM8 in Vitro in a Cu^{2+}-dependent Fashion—ADAM8 produces α-cleavage of MoPrP *in vitro* (7). To identify the specific cleavage point and to evaluate other possible products, $MoPrP^C$ was treated with ADAM8, but without additional reagents that might produce ROS. MoPrP (20 μM) was incubated with 20 ng/μl activated recombinant ADAM8 for 6 h in a low salt pH 7.4 buffer, conditions that minimize MoPrP precipitation (Fig. 3*A*). The resulting cleavage pattern was determined by mass analysis of the individual fragment peaks, followed by correlation of the peptide masses to the cleavage locations in MoPrP. Fragments corresponding to cleavage of MoPrP at the expected site of α-cleavage, Lys-109 ↓ His-110, were observed to within 1 Da of the predicted masses of N1 and C1; this event will henceforth be referred to as α_1-cleavage. Surprisingly, additional fragments were observed corresponding to β-cleavage in the octarepeat domain at Pro-59 ↓ His-60, Pro-67 ↓ His-68, Pro-75 ↓ His-76, and Pro-83 ↓ His-84, as well as a small amount of additional α-cleavage centered on Ala-116 ↓ Ala-117. This latter proteolysis event will be referred to as α_2-cleavage and is somewhat ragged with variation of the cut point by two or three Ala residues. It is interesting to note that Cu^{2+}-mediated ROS produced β-cleavage following each histidine, whereas ADAM8 β-cleavage took place before each histidine. Additional smaller unannotated peaks, which resulted from proteolysis at the two cleavage sites, indicate that both α- and β-cleavage can occur within the same protein molecule.

A primary location for copper binding in PrP^C is in the octarepeat domain, composed of four tandem repeats of the fundamental eight-residue segment PHGGGWGQ (27). Within this domain, Cu^{2+} is taken up with two distinct coordination modes depending on the copper concentrations. At low copper levels, a single Cu^{2+} ion coordinates to the four octarepeat histidines with a K_d of ~0.1 nM. At high copper levels, up to four Cu^{2+} ions are taken up, with one metal ion in each of the repeating PHGGGWGQ sequences (coordinated specifically to the HGGGW subsequence). The affinity is significantly lower, with a K_d of ~10 μM (28). An additional 2 eq of Cu^{2+} are coordinated outside the octarepeat domain by His-95 and His-110 (mouse sequence) with a K_d of ~0.1 nM (25). Alternatively, the octarepeat domain may take up a single Zn^{2+} ion through the four histidines with an affinity of ~200 μM (29).

Given that copper coordinates to PrP^C in segments that are susceptible to proteolysis, we examined the effects of Cu^{2+} on ADAM8 cleavage (Fig. 3*A*). The addition of 2 eq of Cu^{2+} (40 μM), but no ascorbic acid, to the cleavage reaction produced distinct differences in the relative amounts of α_1-, α_2-, and β-cleavage products (Fig. 3*C*). We report only peak integration of C-terminal fragments because co-elution of N-terminal cleavage fragments prevented reliable quantification of the

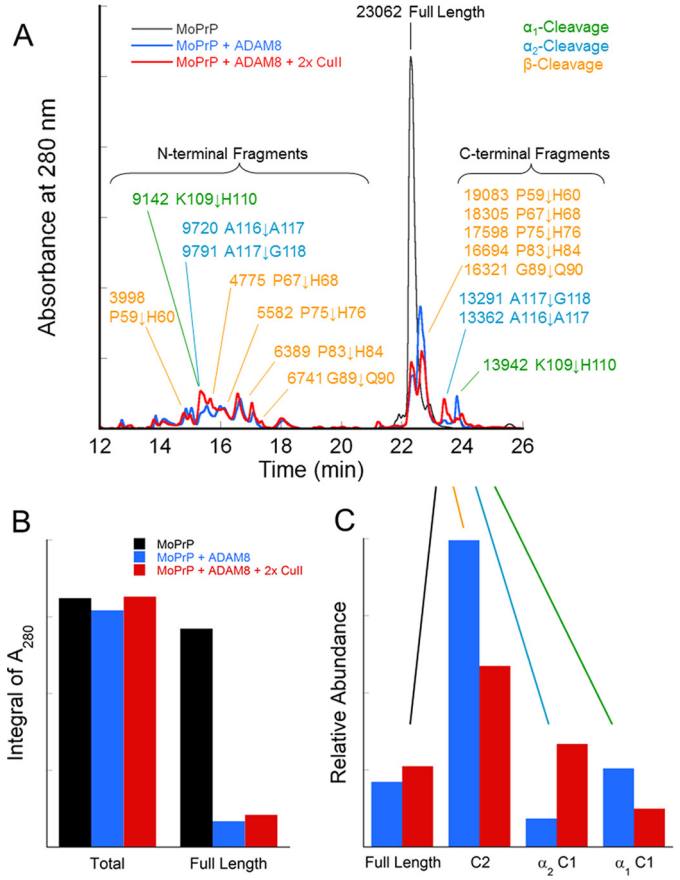

FIGURE 3. **MoPrP is cleaved in multiple locations by ADAM8 in a Cu^{2+}-dependent manner.** *A*, cleavage products of 20 μM MoPrP were analyzed by LC/MS following incubation for 6 h at 37 °C in the absence (*black*) or presence (*blue*) of ADAM8. Similar experiments with ADAM8 and 2 eq of Cu^{2+} (*2× CuII*) are shown in *red*. Peaks are annotated by their masses as well as the location of cleavage corresponding to the observed mass. Peaks corresponding to α_1-cleavage are annotated in *green*, α_2-cleavage in *blue*, and β-cleavage in *orange*. *B*, the A_{280} was integrated for the entire LC trace (*left*) and just the peak corresponding to uncleaved PrP (*right*) for each reaction condition. *C*, the A_{280} of each C-terminal peak generated by cleavage in the absence (*blue*) and presence (*red*) of Cu^{2+} was integrated and then weighted by the corresponding extinction coefficient.

N-terminal peaks. Interestingly, the addition of Cu^{2+} to the cleavage reaction appeared to reduce the amounts of α_1- and β-cleavage while increasing the amount of α_2-cleavage. The percent of reacted MoPrP remained relatively unchanged at >85% with or without the addition of Cu^{2+} (Fig. 3*B*). As a control, the entire LC traces in Fig. 3*A* were integrated to ensure that the total amount of protein observed for each cleavage reaction was approximately the same.

To further understand the role that Cu^{2+} plays in ADAM8 cleavage, we performed a titration from 0 to 8 eq of Cu^{2+} (Fig. 4, *A* and *B*, N- and C-terminal fragments, respectively). In the absence of Cu^{2+}, cleavage was dominated by α_1- and β-cleavage, as noted above. However, the addition of 1 eq of Cu^{2+}, which binds primarily to the octarepeat domain, reduced the amount of C2 protein observed by a factor of 2 while increasing the amounts of both α_1- and α_2-C1 fragments. Additional equivalents of Cu^{2+} resulted in increasing amounts of α_2-C1 while reducing the level of α_1-C1. This suggests that copper coordination at His-110 suppresses α_1-cleavage. We note that because both α- and β-cleavage events can occur on the same peptide, the observed levels of N- and C-terminal fragments do not necessarily match, notably between N2 and C2 fragments.

To evaluate the rate at which ADAM8 cleaves MoPrP, we performed a time trial over the course of 12 h (Fig. 4*C*). Primary cleavage was nearly complete by 4 h; however, the level of C2 continued to drop while the level of α_1-C1 increased, likely due to C2 peptide fragments being subsequently cleaved again at the α_1-site.

Zn^{2+} Modulates ADAM8 Cleavage of MoPrP in a Pattern Different from That of Cu^{2+}—MoPrP is capable of coordinating Zn^{2+} in the octarepeat domain, albeit with a weaker affinity than that for Cu^{2+}. However, extracellular levels of Zn^{2+} are significantly higher compared with Cu^{2+}, suggesting that PrP^C may nevertheless coordinate Zn^{2+} *in vivo* (30). Additionally, PrP^C is involved in zinc uptake into neurons (31). To evaluate whether Zn^{2+} influences ADAM8 cleavage of MoPrP, we performed an ADAM8 cleavage assay with 20 μM MoPrP and 80 μM Zn^{2+} (Fig. 5). MoPrP can coordinate only one Zn^{2+} ion; the added 4 eq are the maximum possible without lowering MoPrP solubility. The addition of Zn^{2+} to the cleavage reaction resulted in a similar reduction of C2 to that seen with Cu^{2+}; however, the relative proportions of α_1- and α_2-C1 were reversed. This suggests that zinc suppresses β-cleavage in the octarepeat domain, where the metal ion is known to bind, but does not influence the proportions of α-cleavage relative to the case with enzyme alone.

Cu^{2+} Modulates ADAM8 α_1-Cleavage of MoPrP through His-110 and α_2-Cleavage through the Octarepeat Domain—The data above suggest that copper coordination to His-110 suppresses α_1-cleavage. To test this hypothesis, we mutated MoPrP His-110 to tyrosine, thereby eliminating Cu^{2+} coordination at that residue. Surprisingly, as opposed to removing the copper blockage to α_1-cleavage, the H110Y mutation actually reduced α_1-cleavage (Fig. 6*A*), which suggests that His is part of the consensus sequence for ADAM8 activity. As with the wild type, the addition of copper reduced β-cleavage and enhanced general α-cleavage, with the latter primarily as α_2-products (Fig. 6*A*).

We next assayed ADAM8 cleavage of MoPrP(90–230), which lacks the N terminus, including the octarepeat domain (Fig. 6*B*). Analysis of the relatively low molecular weight N-terminal cleavage fragments is provided for MoPrP(90–230) experiments due to their superior HPLC separation compared with C-terminal fragments. Although cleavage fragments corresponding to both α_1- and α_2-cleavage were observed in the absence of Cu^{2+}, generally less cleavage was seen as reflected in the amount of unreacted full-length protein. The addition of 2 eq of Cu^{2+} resulted in a decrease in α_1-cleavage, similar to wild-type MoPrP, whereas α_2-cleavage levels were unaffected by the addition Cu^{2+}. Together, these data suggest that α_2-cleavage is enhanced by copper occupation of the octarepeat domain in the wild-type protein, perhaps through a non-local interaction (see "Discussion").

Pathogenic Mutants MoPrP E199K and D177N Exhibit Decreased ADAM8 α_2-Cleavage upon Addition of Cu^{2+} Relative to Wild-type MoPrP—Recent work suggests that Zn^{2+} and Cu^{2+} promote a tertiary interaction between the metal-occupied

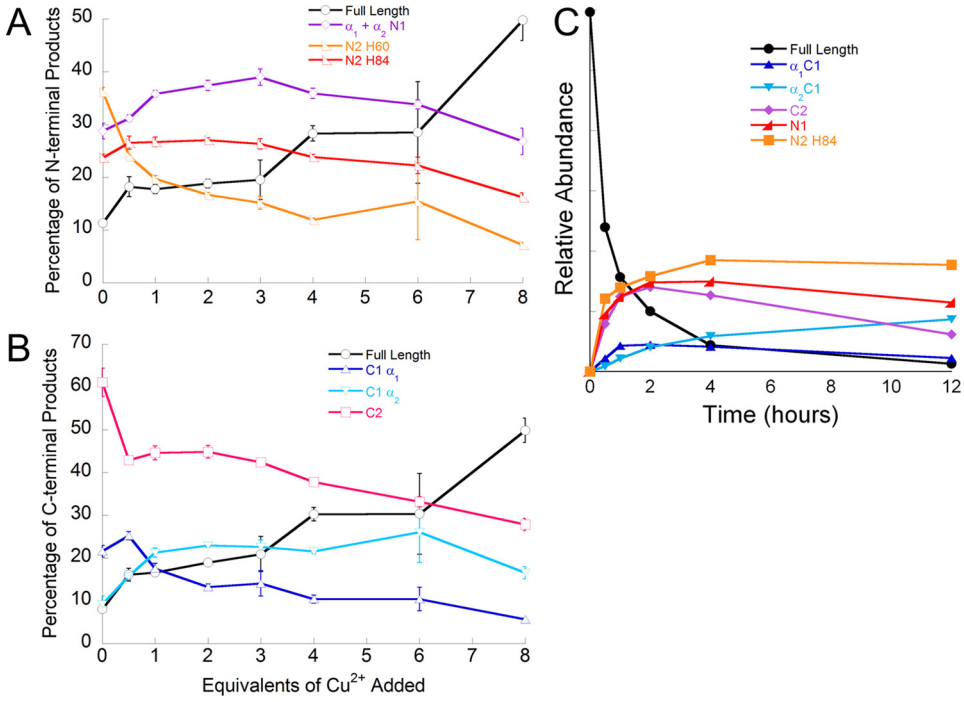

FIGURE 4. **Time and Cu^{2+} modulate ADAM cleavage of MoPrP.** A Cu^{2+} titration of 20 μM MoPrP cleavage by ADAM8 was analyzed by LC/MS. Peaks from the LC trace were integrated and weighted by their corresponding extinction coefficients to obtain the relative abundance of the fragments. Integration values are plotted as a function of Cu^{2+} added *versus* relative abundance for both N-terminal fragments (*A*) and C-terminal fragments (*B*). The N-terminal fragments resulting from α_1- and α_2-cleavage co-eluted, so their combined peaks were integrated, plotted, and labeled ($\alpha_1 + \alpha_2$ *N1*). *N2 H84* and *N2 H60* refer to the N-terminal fragments resulting from cleavage at Pro-83 ↓ His-84 and Pro-59 ↓ His-60, respectively. *C*, time points of ADAM8 cleavage of MoPrP in the absence of Cu^{2+} were taken over the course of 12 h by halting the reaction at the appropriate time with the addition of the ADAM8 inhibitor Batimastat.

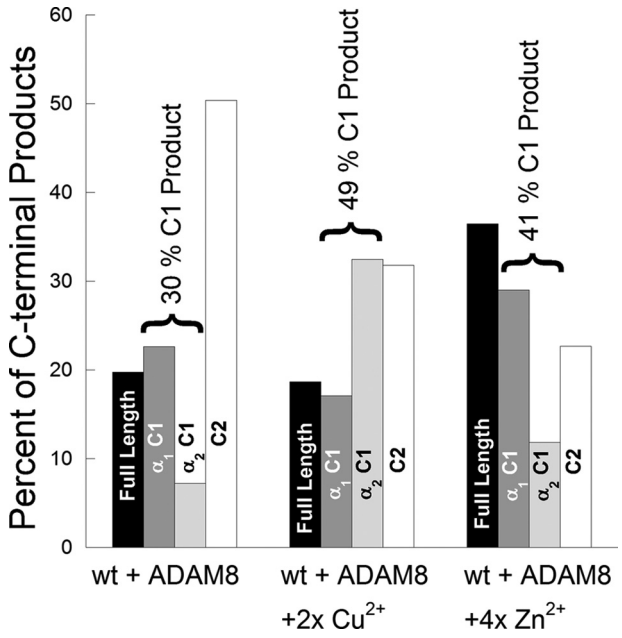

FIGURE 5. **The ADAM8 cleavage pattern of MoPrP is altered by Cu^{2+} and Zn^{2+}.** Cleavage of MoPrP by ADAM8 was assayed by LC/MS in the absence (*left*) and presence of 2 eq of Cu^{2+} (*middle*) or 4 eq of Zn^{2+} (*right*). 280 nm absorbance peaks corresponding to C-terminal cleavage products were integrated and weighted by their respective extinction coefficients to give relative abundance. The abundance of each product was normalized to the total amount of full-length plus C-terminal protein fragments for each reaction condition.

N-terminal octarepeats and the folded C-terminal domain (24, 32). In addition, two C-terminal pathogenic mutants in familial prion disease, MoPrP E199K and D177N, destabilize this interdomain interaction. Because Cu^{2+} modulates α_2-cleavage (see above), we wanted to evaluate the consequence of the E199K and D177N mutations on ADAM8 cleavage with and without added copper. Analysis of ADAM8 cleavage by LC/MS revealed that in the apo-state, MoPrP E199K and D177N behaved like wild-type MoPrP (Fig. 7*A*), with both mutants giving a preponderance of C2 product. When Cu^{2+} was added to both wild-type MoPrP and the mutant species, C2 was suppressed relative to C1; however, the ratios of α_1- and α_2-C1 products depended on the specific protein. As shown in Fig. 7*B*, in the absence of copper (apo-state), the α_2-C1/α_1-C1 product ratio was constant. However, with 2 eq of copper, the mutant species showed systematically less α_2-C1 relative to α_1-C1.

ADAM10 and ADAM17 Cleave MoPrP at a Novel Location, Termed α_3-Cleavage—In addition to ADAM8, both ADAM10 and ADAM17 are implicated in α-cleavage of MoPrP (8). To investigate the role these enzymes play in MoPrP cleavage, we performed the same LC/MS assay we used for ADAM8 with recombinant ADAM10 and ADAM17 (Fig. 8*A*). Analysis for both N- and C-terminal fragments is reported due to good HPLC separation of all fragments. We buffered the cleavage reaction at both physiological pH 7.4 and enzymatically optimal pH 9. After a 6-h reaction, neither ADAM10 nor ADAM17 cleaved MoPrP at the purported site of α-cleavage, Lys-109 ↓ His-110. Instead, the proteases cleaved MoPrP several amino acids more C-terminal at Ala-119 ↓ Val-120, which will be referred to as α_3-cleavage. Additionally, ADAM10 cleaved MoPrP at Gly-227 ↓ Arg-228, which has been previously reported as sheddase activity, releasing PrP from its membrane anchor (9). We refer to the released PrP product as N3. Neither

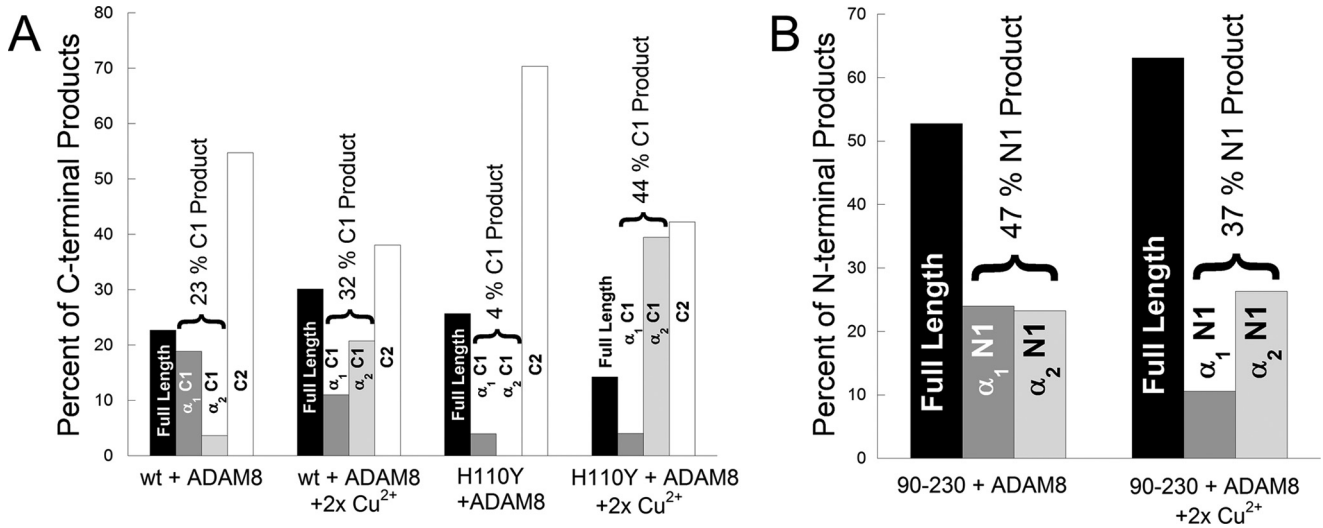

FIGURE 6. **His-110 and the N terminus of MoPrP modulate ADAM8 cleavage of PrP.** *A*, LC/MS analysis of ADAM8 cleavage of MoPrP H110Y revealed that α_1-cleavage was blocked. The addition of 2 eq of Cu^{2+} resulted in increased α_2-cleavage; however, α_1-cleavage remained unchanged. *B*, like wild-type MoPrP, MoPrP(90–230), which lacks the N terminus, experienced the same reduction in α_1-cleavage when 2 eq of Cu^{2+} were added to the ADAM8 cleavage reaction. However, unlike wild-type MoPrP, ADAM8 cleavage of MoPrP(90–230) in the absence of Cu^{2+} produced a significant amount of α_2-cleavage.

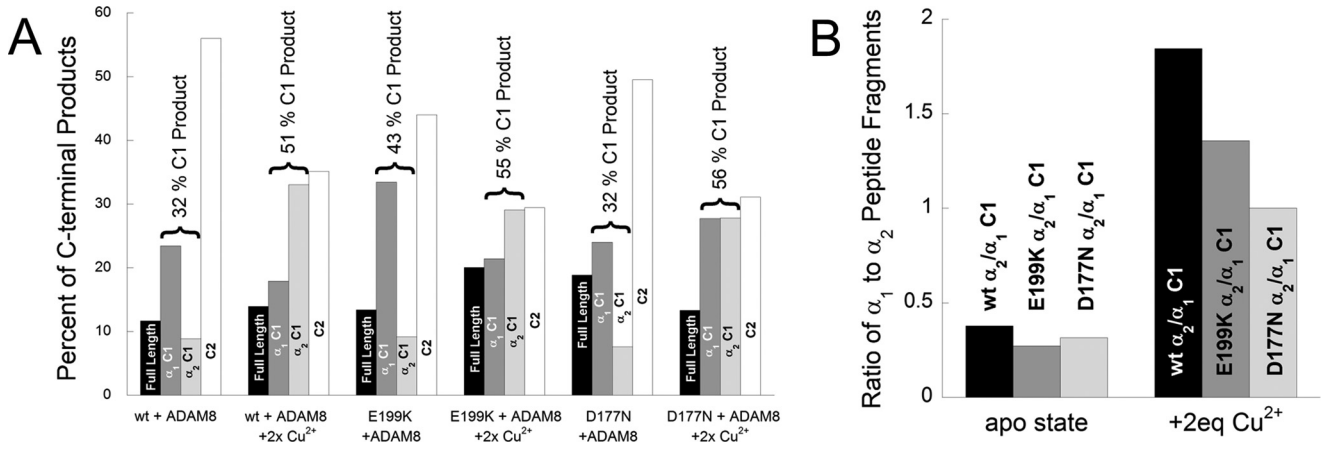

FIGURE 7. **Pathogenic mutants MoPrP E199K and D177N alter the Cu^{2+} regulation of α_2-cleavage.** *A*, ADAM8 cleavage of MoPrP E199K and D177N was assayed by LC/MS. In the absence of Cu^{2+}, both D177N and E199K were cleaved in the same pattern as wild-type MoPrP. *B*, despite similar cleavage patterns seen in *A*, the ratios of α_2-C1 to α_1-C1 peptide in the two mutants were affected by the presence of Cu^{2+}.

Cu^{2+} nor Zn^{2+} affected ADAM10 or ADAM17 cleavage of MoPrP (data not shown).

Given the success of MoPrP H110Y at blocking ADAM8-mediated α_1-cleavage, we sought to create an additional MoPrP mutant that could block ADAM10 and ADAM17 α_3-cleavage. Previous work with peptide libraries has mapped out the contribution of each amino acid in the active site to enhancing or reducing cleavage by ADAM10 and ADAM17 (33). Aspartic acid at any location in the P5 to P4′ position of the cleavage site showed greatly reduced ADAM10 and ADAM17 cleavage; we therefore mutated MoPrP Val-120 to aspartic acid in an attempt to block cleavage at Ala-119 ↓ Val-120. After a 24-h reaction, MoPrP V120D gave an 80–90% reduction in α_3-cleavage from either ADAM10 or ADAM17 (Fig. 8*B*). ADAM10 was still able to cleave MoPrP V120D at Gly-227 ↓ Arg-228, producing N3 at levels comparable to wild-type MoPrP. Using the same strategy, we mutated Arg-228 to aspartic acid to block ADAM10 cleavage at Gly-227 ↓ Arg-228 and the consequent formation of N3. After a 24-h incubation with ADAM10, we saw no cleavage at Gly-227 ↓ Asp-228, whereas ADAM10 cleavage at Ala-119 ↓ Val-120 remained unaffected. These findings show that the strategy of $X \rightarrow$ Asp mutation successfully blocks selective ADAM10/ADAM17 activity.

Embryonic Lethal MoPrP Mutant ΔCR Lacking Residues 105–125 Produces Alternative Cleavage Patterns When Exposed to ADAM8, ADAM10, and ADAM17—Although MoPrP knock-out mice are viable, mice expressing a MoPrP mutant with residues 105–125 deleted (MoPrP ΔCR) do not reach maturity (Ref. 34; see also the work of Baumann *et al.* (35), in which residues 94–134 were deleted). The reasons for the lethal phenotype are not known, although it has been proposed that amino acids 105–125 of MoPrP are critical for an interaction with a potential PrP binding partner (34). Given our findings that ADAM8, ADAM10, and ADAM17 all cleave MoPrP within this region, we hypothesized that MoPrP ΔCR would alter all forms of α-cleavage. We therefore determined the cleavage patterns for MoPrP ΔCR mediated by all three proteases (Fig. 9). Wild-type MoPrP cleaved by ADAM8 underwent α_1-, α_2-, and β-cleavage;

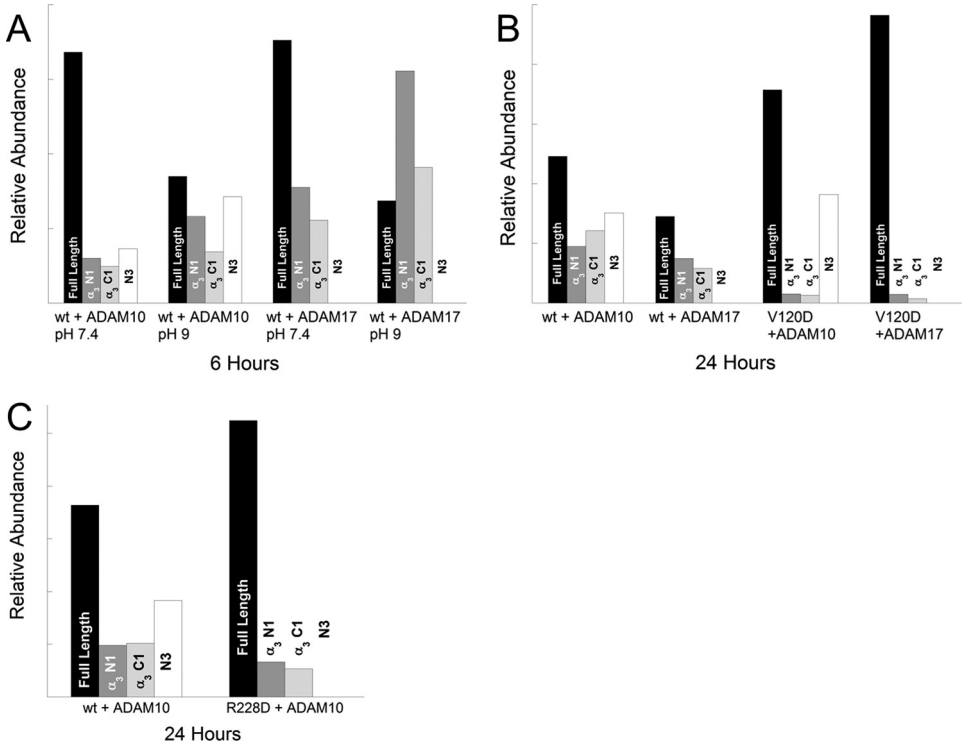

FIGURE 8. **ADAM10 and ADAM17 both cleave MoPrP at Ala-119 ↓ Val-120.** *A*, MoPrP was reacted with ADAM10 and ADAM17 at both pH 7.4 and enzymatically optimal pH 9. ADAM10 and ADAM17 cleaved MoPrP at Ala-119 ↓ Val-120, producing α_3-N1 and α_3-C1. ADAM10 also cleaved MoPrP at Gly-227 ↓ Arg-228, producing the N3 fragment. *B*, even after 24 h, the mutant MoPrP V120D experienced greatly reduced α_3-cleavage by both ADAM10 and ADAM17 at pH 7.4. ADAM10 cleavage at Gly-227 ↓ Arg-228 remained at levels comparable to those of wild-type MoPrP. *C*, cleavage near the C terminus releasing the N3 fragment was ablated in MoPrP R228D, whereas cleavage at Ala-119 ↓ Val-120 was unaffected.

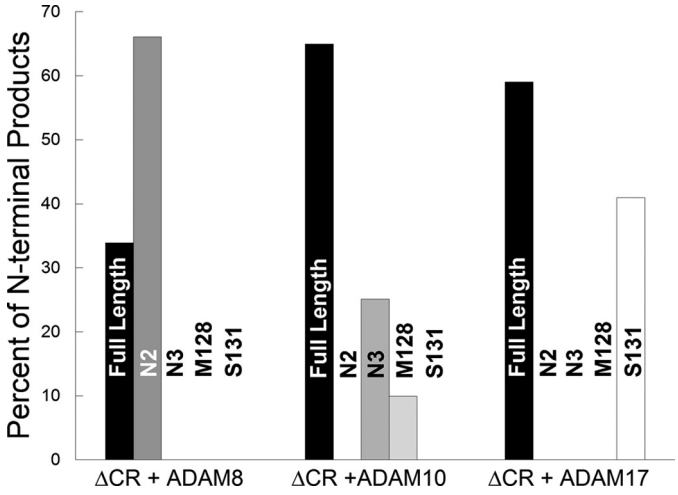

FIGURE 9. **PrP ΔCR does not produce α_1-, α_2-, or α_3-cleavage fragments.** PrP ΔCR was reacted with ADAM8 (*left*), ADAM10 (*middle*), or ADAM17 (*right*). The relative abundance of N-terminal cleavage fragments is shown. ADAM8 still cleaved ΔCR within the octarepeat domain (N2), but no α_1- or α_2-cleavage was observed. ADAM10 cleaved ΔCR at Gly-227 ↓ Arg-228 (wild-type amino acid indexing), producing the N3 fragment, but cleavage at Ala-119 ↓ Val-120 was abolished. Instead, a small amount of peptide fragment corresponding to cleavage at Tyr-127 ↓ Met-128 was observed. ADAM17 also did not cleave ΔCR at Ala-119 ↓ Val-120 but instead at Gly-130 ↓ Ser-131.

however, MoPrP ΔCR, lacking the α_1- and α_2-cleavage sites, showed only β-cleavage as reflected by the N2 product. ADAM10 maintained cleavage of MoPrP ΔCR near the C terminus (N3 product); however, no fragments corresponding to α_3-cleavage were observed. Instead, a small amount of peptide resulting from cleavage at Tyr-127 ↓ Met-128 was produced (wild-type MoPrP sequence). Likewise, ADAM17 gave an alternative cleavage location at Gly-130 ↓ Ser-131. The new cleavage locations from ADAM10 and ADAM17 are both quite close to the deleted region, but the efficiency is low relative to the wild type.

DISCUSSION

α-Cleavage and β-cleavage of PrP^C are important proteolytic processing events that release bioactive protein fragments. With few exceptions (7, 9, 36), the identification of PrP^C cleavage products has been determined by Western blotting, which lacks the power to resolve fragment masses at atomic mass unit resolution. Subtle differences in fragment masses may not be distinguishable, leading to low resolution and perhaps an oversimplified understanding of PrP^C processing. Here, we applied LC/MS to evaluate the detailed reactions of copper/ascorbate, ADAM8, ADAM10, and ADAM17 on full-length PrP^C to systematically analyze MoPrP cleavage fragments.

Our primary findings are encapsulated with the following observations: 1) Combined ascorbic acid and Cu^{2+} generate ROS that cleave MoPrP within the octarepeat domain (β-cleavage). 2) ADAM8 cleaves MoPrP at H110Y, the previously identified location of α-cleavage in brain extract. Additional cleavage is also observed around Ala-116 (α_2-cleavage) and within the octarepeat domain (β-cleavage) in a Cu^{2+}- and Zn^{2+}-dependent fashion. 3) ADAM10 and ADAM17 cleave MoPrP at Val-120, and ADAM10 also cleaves MoPrP at Arg-228, which releases the protein from its membrane anchor. 4) The toxic mutants MoPrP E199K and D177N (mouse numbering) and

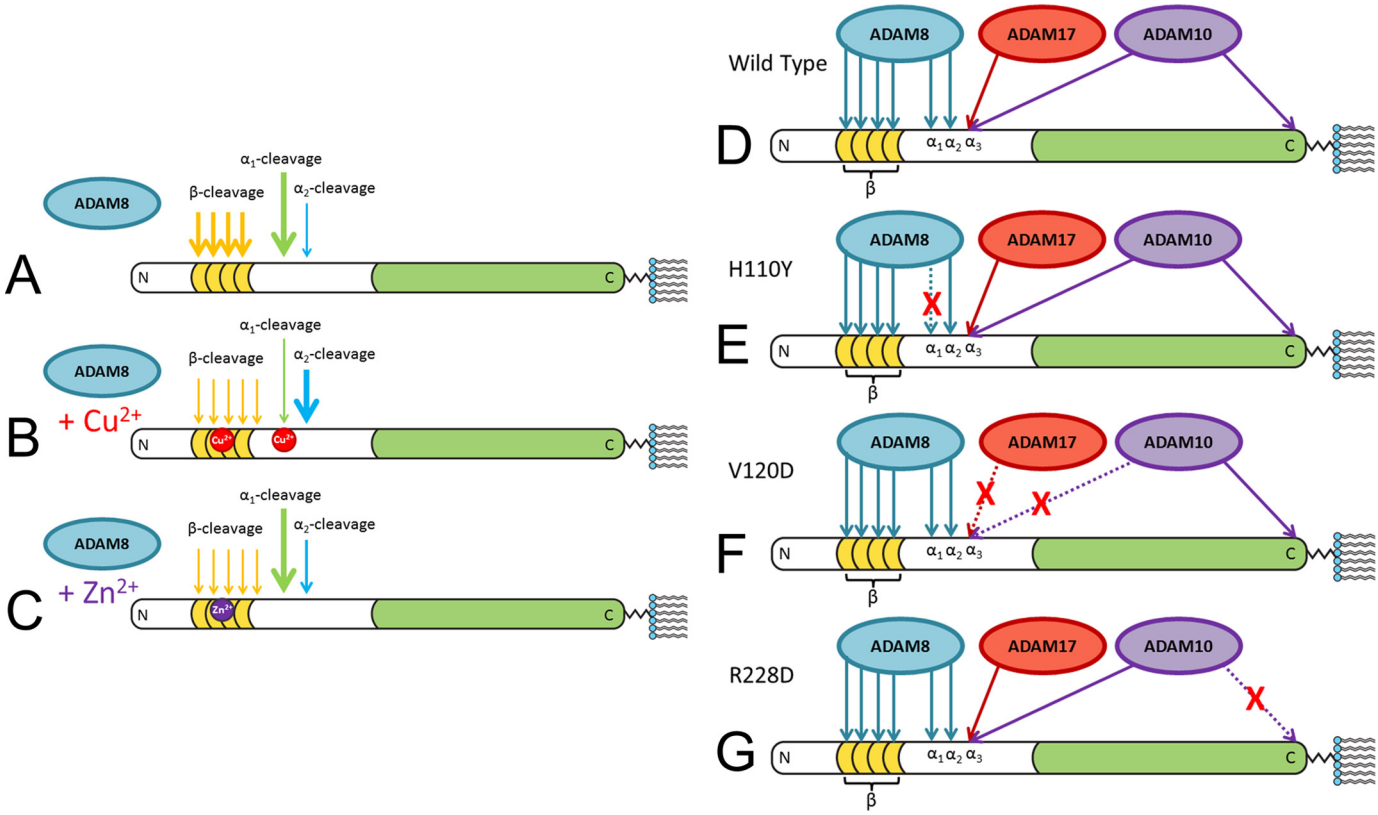

FIGURE 10. **Schematic of PrP cleavage.** The octarepeat domain (*gold*), the folded C-terminal domain (*green*), and C-terminal GPI anchor are shown. *A*, ADAM8 cleaves PrP both in the octarepeat domain (β-cleavage) and at Lys-109 ↓ His-110 (α_1-cleavage). The *arrow thickness* correlates to relative cleavage activity. *B*, upon addition of 2 eq of Cu^{2+}, β-cleavage and α_1-cleavage are diminished, whereas α_2-cleavage is enhanced. *C*, the addition of Zn^{2+} results in diminished β-cleavage while maintaining similar levels of α_1-cleavage relative to the apo-state. *D*, ADAM8, ADAM10, and ADAM17 all cleave MoPrP at distinct locations. The only overlap is at the α_3-location, where both ADAM10 and ADAM17 cleave. *E*, the MoPrP mutant H110Y blocks ADAM8 cleavage at Lys-109 ↓ Tyr-110 (α_1-cleavage). *F*, the MoPrP mutant V120D blocks ADAM10 and ADAM17 cleavage at Ala-119 ↓ Asp-120 (α_3-cleavage); however, the ability of ADAM10 to cleave MoPrP V120D at Gly-227 ↓ Arg-228 remains unaffected. *G*, MoPrP R228D blocks ADAM10 cleavage at Gly-227 ↓ Asp-228 (resulting in the N3 fragment); however, ADAM10 still cleaves MoPrP R228D at Ala-119 ↓ Val-120.

MoPrP ΔCR all produce altered ADAM cleavage patterns. Notably, the cleavage patterns observed for E199K and D177N are influenced by the presence of Cu^{2+}. 5) The H110Y, V120D, and R228D mutants block ADAM cleavage at their respective locations.

Our results are summarized in Fig. 10. Experiments involving ADAM8 are detailed on the *left*. The thickness of the arrows corresponds to the relative levels of cleavage yield at the indicated locations in the absence and presence of Cu^{2+} and Zn^{2+}. The overall cleavage locations for ADAM8, ADAM10, and ADAM17 are depicted on the *right*. Additionally, *dashed lines* denote those cleavage locations blocked by our engineered MoPrP mutants.

Current thinking holds that PrP^C undergoes α- and β-cleavage by distinct mechanisms. α-Cleavage is a normal processing event observed in brain extract that occurs between Lys-109 and His-110, likely resulting from the action of ADAM8, ADAM10, or ADAM17. However, β-cleavage is an aberrant reaction, seen at abnormally high levels in Creutzfeldt-Jakob disease brain extract, and results from the copper-mediated production of ROS that chemically cleave the polypeptide backbone at the end of the octarepeat domain. Our findings suggest a revision of this elementary scheme. First, we found that β-cleavage may also be enzymatic, with ADAM8 acting with equivalent efficiency at the α- and β-sites. Moreover, ADAM8-driven β-cleavage does not correspond to a single site but instead takes place between each Pro-His bond in the octarepeat domain. Second, in the absence of a reducing agent, we found that copper actually suppresses β-cleavage. We propose that by binding with high affinity to N-terminal His residues within the octarepeat and at His-110, Cu^{2+} prevents the polypeptide substrate from entering the enzyme active site, thereby suppressing β- and α_1-cleavage, respectively. Zn^{2+} binds only to the octarepeat domain and accordingly suppresses only β-cleavage. Finally, we found that α-cleavage does not take place at a single site but instead occurs at one of three nearby sites depending on the specific enzyme. ADAM8 produces α_1- and α_2-cleavage, preceding His-110 and Ala-117 (palindromic region), respectively, whereas ADAM10 and ADAM17 produce α_3-cleavage at Val-120. α-Cleavage occurring at multiple sites provides an explanation for why the entire palindromic region of PrP^C had to be deleted to fully block cleavage *in vivo* (12). Deletions of shorter regions that encompass only α_1, α_2, or α_3 only partially suppressed cleavage.

Spevacek *et al.* (24) discovered a novel N-terminal/C-terminal interaction in PrP^C promoted by zinc. Specifically, Zn^{2+} binds to the octarepeat domain, which then docks against a conserved negatively charged C-terminal surface formed by helices 2 and 3. Pathogenic mutations localized to these helices tend to reduce the strength of this tertiary interaction. The

proteolysis results reported here suggest that the zinc-induced fold increases the sensitivity to α_2-cleavage (Fig. 5). As shown in Fig. 6*A*, the addition of 2 eq of Cu^{2+} to wild-type PrP^C (with 1 eq taken up in the octarepeat domain with His coordination like that of Zn^{2+}) promotes α_2-cleavage. However, this effect is muted in PrP(90–230) (Fig. 6*B*), which lacks the octarepeat domain. Moreover, PrP^C with pathogenic mutations (Fig. 7*B*) exhibits a decrease in α_2-cleavage relative to α_1-cleavage but only in the presence of Cu^{2+}. These data suggest that the tertiary structure promoted by metal ion coordination exposes the palindromic region of PrP^C, which resides between the octarepeats and the folded C-terminal domain, thereby enhancing α_2-cleavage.

It is interesting to consider PrP^C as a proprotein, with α-cleavage required to release the active N1 peptide. Evolving literature from the Checler laboratory (13) shows that N1 is protective and acts by suppressing apoptosis, possibly through inhibition of caspase-3 or other pro-apoptotic agents. The mechanism by which extracellular N1 affects these intracellular processes is unknown but apparently does not require N1 internalization. The N1 peptide may also play an important role in slowing the progression of Alzheimer disease. Harris and colleagues (37) demonstrated that N1 binds with high affinity to Aβ oligomers, thereby reducing Aβ toxicity in neuron culture and animal assays. Aβ oligomer binding takes place at two locations in N1: residues 23–31 and 95–105. All α-cleavage points identified by our studies are C-terminal of segment 95–105 and likely preserve Aβ affinity among the three N1 variants. However, this has not been directly tested. Copper was previously linked to β-cleavage, which produces N2 lacking residues 95–105 and thus might be considered as a species that enhances the events leading to Aβ-driven neurodegeneration. However, our findings here suggest a different scenario. As summarized in Fig. 10, both copper (under nonreducing conditions) and zinc suppress β-cleavage, and copper enhances α_2-cleavage. Consequently, these metal ions may be important regulators in the production of N1. If so, our findings may help explain the often conflicting results of copper chelation therapies in the treatment of Alzheimer disease (38–41).

PrP^C is found in various biologically active forms: full-length protein anchored to the extracellular membrane, released full-length protein shed from the membrane, α-cleaved protein (N1 and C1 fragments), and β-cleaved protein (N2 and C2 fragments). At the present time, there is little understanding with regard to how alteration in cleavage patterns plays into general PrP^C function and prion disease. For example, as noted above, the lethality of MoPrP ΔCR is attributed to a loss of molecular recognition of an unknown PrP^C binding partner (34) or through promotion of spontaneous ion channeling (42). However, it is also possible that deletion of the CR region, which spans the α_1-, α_2-, and α_3-cleavage sites, exerts its lethal phenotype by fully blocking native α-cleavage. In this scenario, released N1 may be essential for myelination and other components of neurological development. Similarly, proteolytic sheddase activity (as distinct from GPI anchor cleavage) may be important for maintaining levels of free PrP^C, with potential roles in neuron development and maintenance (10, 23). In our work here, beyond identification of specific enzyme cleavage sites, we also developed and tested $X \rightarrow$ Tyr or Asp point mutations that selectively inhibit ADAM8, ADAM10, and ADAM17 proteolysis, thus suppressing α_1-cleavage, sheddase, and α_3-cleavage, respectively. In cellular and transgenic animal studies, these mutants could serve as important new tools for assessing the relative roles of PrP^C cleavage products.

Acknowledgment—We are grateful to Ann Spevacek for providing several proteins used in this study.

REFERENCES

1. Bolton, D. C., McKinley, M. P., and Prusiner, S. B. (1982) Identification of a protein that purifies with the scrapie prion. *Science* **218,** 1309–1311
2. Riek, R., Hornemann, S., Wider, G., Billeter, M., Glockshuber, R., and Wüthrich, K. (1996) NMR structure of the mouse prion protein domain PrP(121–231). *Nature* **382,** 180–182
3. Prusiner, S. B. (1998) Prions. *Proc. Natl. Acad. Sci. U.S.A.* **95,** 13363–13383
4. Williams, E. S., and Young, S. (1980) Chronic wasting disease of captive mule deer: a spongiform encephalopathy. *J. Wildl. Dis.* **16,** 89–98
5. Harris, D. A., Huber, M. T., van Dijken, P., Shyng, S. L., Chait, B. T., and Wang, R. (1993) Processing of a cellular prion protein: identification of N- and C-terminal cleavage sites. *Biochemistry* **32,** 1009–1016
6. Chen, S. G., Teplow, D. B., Parchi, P., Teller, J. K., Gambetti, P., and Autilio-Gambetti, L. (1995) Truncated forms of the human prion protein in normal brain and in prion diseases. *J. Biol. Chem.* **270,** 19173–19180
7. Liang, J., Wang, W., Sorensen, D., Medina, S., Ilchenko, S., Kiselar, J., Surewicz, W. K., Booth, S. A., and Kong, Q. (2012) Cellular prion protein regulates its own α-cleavage through ADAM8 in skeletal muscle. *J. Biol. Chem.* **287,** 16510–16520
8. Vincent, B., Paitel, E., Saftig, P., Frobert, Y., Hartmann, D., De Strooper, B., Grassi, J., Lopez-Perez, E., and Checler, F. (2001) The disintegrins ADAM10 and TACE contribute to the constitutive and phorbol ester-regulated normal cleavage of the cellular prion protein. *J. Biol. Chem.* **276,** 37743–37746
9. Taylor, D. R., Parkin, E. T., Cocklin, S. L., Ault, J. R., Ashcroft, A. E., Turner, A. J., and Hooper, N. M. (2009) Role of ADAMs in the ectodomain shedding and conformational conversion of the prion protein. *J. Biol. Chem.* **284,** 22590–22600
10. Altmeppen, H. C., Prox, J., Puig, B., Kluth, M. A., Bernreuther, C., Thurm, D., Jorissen, E., Petrowitz, B., Bartsch, U., De Strooper, B., Saftig, P., and Glatzel, M. (2011) Lack of a-disintegrin-and-metalloproteinase ADAM10 leads to intracellular accumulation and loss of shedding of the cellular prion protein *in vivo*. *Mol. Neurodegener.* **6,** 36
11. Wik, L., Klingeborn, M., Willander, H., and Linne, T. (2012) Separate mechanisms act concurrently to shed and release the prion protein from the cell. *Prion* **6,** 498–509
12. Oliveira-Martins, J. B., Yusa, S., Calella, A. M., Bridel, C., Baumann, F., Dametto, P., and Aguzzi, A. (2010) Unexpected tolerance of α-cleavage of the prion protein to sequence variations. *PLoS ONE* **5,** e9107
13. Guillot-Sestier, M.-V., Sunyach, C., Druon, C., Scarzello, S., and Checler, F. (2009) The α-secretase-derived N-terminal product of cellular prion, N1, displays neuroprotective function *in vitro* and *in vivo*. *J. Biol. Chem.* **284,** 35973–35986
14. Sunyach, C., Cisse, M. A., da Costa, C. A., Vincent, B., and Checler, F. (2007) The C-terminal products of cellular prion protein processing, C1 and C2, exert distinct influence on p53-dependent staurosporine-induced caspase-3 activation. *J. Biol. Chem.* **282,** 1956–1963
15. Westergard, L., Turnbaugh, J. A., and Harris, D. A. (2011) A naturally occurring C-terminal fragment of the prion protein (PrP) delays disease and acts as a dominant-negative inhibitor of PrP^{Sc} formation. *J. Biol. Chem.* **286,** 44234–44242
16. Campbell, L., Gill, A. C., McGovern, G., Jalland, C. M. O., Hopkins, J., Tranulis, M. A., Hunter, N., and Goldmann, W. (2013) The PrP^C C1 fragment derived from the ovine $A_{136}R_{154}R_{171}$ *PRNP* allele is highly abundant in sheep brain and inhibits fibrillisation of full-length PrP^C protein *in vitro*.

Biochim. Biophys. Acta **1832,** 826–836
17. McMahon, H. E., Mangé, A., Nishida, N., Créminon, C., Casanova, D., and Lehmann, S. (2001) Cleavage of the amino terminus of the prion protein by reactive oxygen species. *J. Biol. Chem.* **276,** 2286–2291
18. Watt, N. T., Taylor, D. R., Gillott, A., Thomas, D. A., Perera, W. S., and Hooper, N. M. (2005) Reactive oxygen species-mediated β-cleavage of the prion protein in the cellular response to oxidative stress. *J. Biol. Chem.* **280,** 35914–35921
19. Yadavalli, R., Guttmann, R. P., Seward, T., Centers, A. P., Williamson, R. A., and Telling, G. C. (2004) Calpain-dependent endoproteolytic cleavage of PrP^{Sc} modulates scrapie prion propagation. *J. Biol. Chem.* **279,** 21948–21956
20. Dron, M., Moudjou, M., Chapuis, J., Salamat, M. K., Bernard, J., Cronier, S., Langevin, C., and Laude, H. (2010) Endogenous proteolytic cleavage of disease-associated prion protein to produce C2 fragments is strongly cell- and tissue-dependent. *J. Biol. Chem.* **285,** 10252–10264
21. Chen, S., Yadav, S. P., and Surewicz, W. K. (2010) Interaction between human prion protein and amyloid-β (Aβ) oligomers. Role of N-terminal residues. *J. Biol. Chem.* **285,** 26377–26383
22. You, H., Tsutsui, S., Hameed, S., Kannanayakal, T. J., Chen, L., Xia, P., Engbers, J. D. T., Lipton, S. A., Stys, P. K., and Zamponi, G. W. (2012) Aβ neurotoxicity depends on interactions between copper ions, prion protein, and *N*-methyl-D-aspartate receptors. *Proc. Natl. Acad. Sci. U.S.A.* **109,** 1737–1742
23. Kanaani, J., Prusiner, S. B., Diacovo, J., Baekkeskov, S., and Legname, G. (2005) Recombinant prion protein induces rapid polarization and development of synapses in embryonic rat hippocampal neurons *in vitro*. *J. Neurochem.* **95,** 1373–1386
24. Spevacek, A. R., Evans, E. G. B., Miller, J. L., Meyer, H. C., Pelton, J. G., and Millhauser, G. L. (2013) Zinc drives a tertiary fold in the prion protein with familial disease mutation sites at the interface. *Structure* **21,** 236–246
25. Walter, E. D., Stevens, D. J., Spevacek, A. R., Visconte, M. P., Dei Rossi, A., and Millhauser, G. L. (2009) Copper binding extrinsic to the octarepeat region in the prion protein. *Curr. Protein Pept. Sci.* **10,** 529–535
26. Studier, F. W. (2005) Protein production by auto-induction in high-density shaking cultures. *Protein Expr. Purif.* **41,** 207–234
27. Brown, D. R., Qin, K., Herms, J. W., Madlung, A., Manson, J., Strome, R., Fraser, P. E., Kruck, T., von Bohlen, A., Schulz-Schaeffer, W., Giese, A., Westaway, D., and Kretzschmar, H. (1997) The cellular prion protein binds copper *in vivo*. *Nature* **390,** 684–687
28. Walter, E. D., Chattopadhyay, M., and Millhauser, G. L. (2006) The affinity of copper binding to the prion protein octarepeat domain: evidence for negative cooperativity. *Biochemistry* **45,** 13083–13092
29. Walter, E. D., Stevens, D. J., Visconte, M. P., and Millhauser, G. L. (2007) The prion protein is a combined zinc and copper binding protein: Zn^{2+} alters the distribution of Cu^{2+} coordination modes. *J. Am. Chem. Soc.* **129,** 15440–15441
30. Watt, N. T., and Hooper, N. M. (2003) The prion protein and neuronal zinc homeostasis. *Trends Biochem. Sci.* **28,** 406–410
31. Watt, N. T., Taylor, D. R., Kerrigan, T. L., Griffiths, H. H., Rushworth, J. V., Whitehouse, I. J., and Hooper, N. M. (2012) Prion protein facilitates uptake of zinc into neuronal cells. *Nat. Commun.* **3,** 1134
32. Thakur, A. K., Srivastava, A. K., Srinivas, V., Chary, K. V. R., and Rao, C. M. (2011) Copper alters aggregation behavior of prion protein and induces novel interactions between its N- and C-terminal regions. *J. Biol. Chem.* **286,** 38533–38545
33. Caescu, C. I., Jeschke, G. R., and Turk, B. E. (2009) Active-site determinants of substrate recognition by the metalloproteinases TACE and ADAM10. *Biochem. J.* **424,** 79–88
34. Li, A., Christensen, H. M., Stewart, L. R., Roth, K. A., Chiesa, R., and Harris, D. A. (2007) Neonatal lethality in transgenic mice expressing prion protein with a deletion of residues 105–125. *EMBO J.* **26,** 548–558
35. Baumann, F., Tolnay, M., Brabeck, C., Pahnke, J., Kloz, U., Niemann, H. H., Heikenwalder, M., Rülicke, T., Bürkle, A., and Aguzzi, A. (2007) Lethal recessive myelin toxicity of prion protein lacking its central domain. *EMBO J.* **26,** 538–547
36. Mangé, A., Béranger, F., Peoc'h, K., Onodera, T., Frobert, Y., and Lehmann, S. (2004) α- and β-cleavages of the amino-terminus of the cellular prion protein. *Biol. Cell* **96,** 125–132
37. Fluharty, B. R., Biasini, E., Stravalaci, M., Sclip, A., Diomede, L., Balducci, C., La Vitola, P., Messa, M., Colombo, L., Forloni, G., Borsello, T., Gobbi, M., and Harris, D. A. (2013) An N-terminal fragment of the prion protein binds to amyloid-β oligomers and inhibits their neurotoxicity *in vivo*. *J. Biol. Chem.* **288,** 7857–7866
38. Budimir, A. (2011) Metal ions, Alzheimer's disease and chelation therapy. *Acta Pharm.* **61,** 1–14
39. Kenche, V. B., and Barnham, K. J. (2011) Alzheimer's disease & metals: therapeutic opportunities. *Br. J. Pharmacol.* **163,** 211–219
40. Deibel, M. A., Ehmann, W. D., and Markesbery, W. R. (1996) Copper, iron, and zinc imbalances in severely degenerated brain regions in Alzheimer's disease: possible relation to oxidative stress. *J. Neurol. Sci.* **143,** 137–142
41. Faller, P. (2012) Copper in Alzheimer disease: too much, too little, or misplaced? *Free Radic. Biol. Med.* **52,** 747–748
42. Solomon, I. H., Huettner, J. E., and Harris, D. A. (2010) Neurotoxic mutants of the prion protein induce spontaneous ionic currents in cultured cells. *J. Biol. Chem.* **285,** 26719–26726